Available online at www.sciencedirect.com
SCIENCE DIRECT®
PERGAMON
Polyhedron 22 (2003) 2111–2123
POLYHEDRON
www.elsevier.com/locate/poly

Malonic acid: a multi-modal bridging ligand for new architectures and properties on molecule-based magnets

Catalina Ruiz-Pérez [a,*], Yolanda Rodríguez-Martín [a], María Hernández-Molina [a], Fernando S. Delgado [a], Jorge Pasán [a], Joaquín Sanchiz [b], Francesc Lloret [c], Miguel Julve [c]

[a] *Laboratorio de Rayos X y Materiales Moleculares, Departamento de Física Fundamental II, Universidad de La Laguna, Avda. Astrofísico Francisco Sánchez s/n, 38204 La Laguna, Tenerife, Spain*
[b] *Departamento de Química Inorgánica, Universidad de La Laguna, La Laguna, Tenerife, Spain*
[c] *Facultat de Quimica, Departament de Quimica Inorgànica, Institut de Ciencia Molecular, Universitat de València, València, Spain*

Received 6 October 2002; accepted 24 March 2003

In memory of Prof. Oliver Kahn

Abstract

In this work, we show how the design of one-, two- and three-dimensional materials can strongly benefit from the use of crystal engineering techniques, which can give rise to structures of different shapes, and how these differences can give rise to different properties. We will focus on the networks constructed by assembling malonate ligands and metal centres. The idea of using malonate (dianion of propanedioic acid, H_2mal) is that they can give rise to different coordination modes with the metal ions bind. Extended magnetic networks of dimensionalities 1 (1D), 2 (2D) and 3 (3D) can be chemically constructed from malonato-bridged metallic complexes. These coordination polymers behave as ferro-, ferri- or canted antiferromagnets. The control of the spatial arrangement of the magnetic building blocks is of paramount importance in determining the strength of the magnetic interaction. It depends on the coordination bond between the metal ion and the ligands, and on supramolecular interactions such as stacking interactions or hydrogen bonds.

Keywords: Malonate; Caboxylate; Magnetic properties; Molecular magnetism

1. Introduction

The design of synthetic pathways to obtain systems with desired properties continues to be a challenge for inorganic chemists. In this context, a great interest has been devoted to the development of rational synthetic routes to novel polynuclear compounds of tuneable dimensionality which may have applications as molecular-based magnetic materials [1–3]. Focusing on the approach of having transition metals as spin carriers, it is the declared target to optimise the number of chemical links between the magnetic centres in order to gain an increased contribution from intramolecular interactions and at the same time, to diminish the influence of the weaker intermolecular contacts.

Along this line, many recent reports have focused on the synthesis and structural characterisation of polymeric transition metal compounds using malonate (mal) [4–9] as blocking and bridging ligand. The use of malonate as bridging ligand in metal complexes has shown the versatility of this ligand [4–9]. The structural complexity diversity of the malonato complexes is due to the versatility of this dicarboxylate ligand which can adopt several chelating bidentate and/or different car-

Abbreviations: H_2mal, malonic acid; bipym, 2,2′-bipyrimidine; phen, phenantroline; Im, imidazole; MeIm, methylimidazole; 2,4′-bipy, 2,4′-bipyridine; 4,4′-bipy, 4,4′-bipyridine; bpy, 2,2′-bipyridine; pyz, pyrazine; pym, pyrimidine.

* Corresponding author. Tel.: +34-922-318-236; fax: +34-922-318-320.
E-mail address: caruiz@ull.es (C. Ruiz-Pérez).

0277-5387/03/$ - see front matter
doi:10.1016/S0277-5387(03)00303-6

boxylato-bridging coordination modes. The ability of the carboxylato bridge to mediate significant ferro- or antiferromagnetic coupling [10–14] between the paramagnetic centres enhances the interest in the malonate ligand, aiming at designing extended magnetic systems. Additionally, the carboxylate group provides an efficient pathway that couples the magnetic centres either ferro- or antiferromagnetically [10–14], the coupling constant being influenced by structural aspects such as the conformation of the bridge or the geometry of the metal environment.

The malonate ligand is a dicarboxylic ligand with a singular behaviour different from the other dicarboxylic ligands. In our investigations, we have observed that with 3D ions it can exhibit different coordination modes such as (a) bidentate [η^5-chelation], (b) bidentate [η^5-chelation]+unidentate and (c) bidentate [η^5-chelation]+bis(unidentate).

The malonate ligand occupies one or two coordination positions and neutralises two positive charges of the metallic ion, allowing the inclusion of other ligands in the coordination sphere of the metal. These complementary ligands can act as bridging or blocking ligands, contributing to the interconnection or isolation of the spin carriers. Thus, combining the malonate with other bridging and/or blocking ligands we have been able to prepare monomers, dimers, trimers, tetramers, infinite chains, and 2D and 3D arrays.

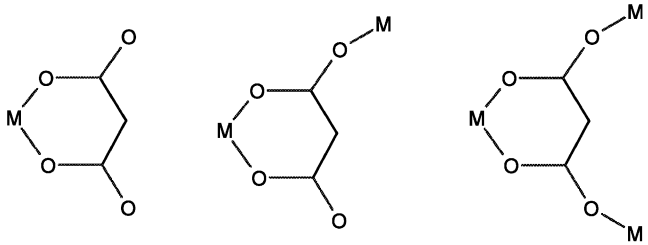

Another feature of the carboxylato bridge is the fact that the magnitude of the exchange interaction depends on the possible *syn–syn*, *syn–anti* and *anti–anti* bridging modes that it can adopt. The nature (ferro- or antiferromagnetic) of the interaction being dependent on the nature of the magnetic orbitals of the spin carriers connected by the bridging ligand. In our compounds, these features are nicely in line with theoretical models developed in molecular magnetism, in particular as far as the symmetry rules involving the magnetic orbitals. Thus, playing with the stoichiometry and with the nature of other complementary ligands, very smart several compounds with a controlled dimensionality and with a nicely explained satisfactory explanation of their magnetic properties have been prepared.

Herein, we present an overview of our investigations in the magneto-structural correlations of malonato complexes. This study is organised attending to the coordination modes of the malonate and how they govern the dimensionality of the structure, then the magnetic properties can be explained attending to the bridging mode of the carboxylate and the nature of the magnetic orbital of the paramagnetic centres.

2. Structural aspects and magnetic properties

2.1. Bidentate (no-bridging)

In this coordination mode two of the oxygens of the malonate coordinate the metal ion, the ligand behaving as η^5-bidentate, the rest of the oxygens may act as acceptors in hydrogen bonding. This mode is analogue to the η^4-bidentate chelate exhibited by the oxalate. The malonate acts as blocking ligand leading to isolated molecules that are interconnected through hydrogen bonding, exhibiting weak or no magnetic coupling among the metallic centres [15,16].

As examples, we have the bimetallic compounds $[M^{II}(H_2O)_6][Cu^{II}(mal)_2(H_2O)_2]$ (**1**) (M = Mn, Co, Ni, Cu and Zn) [17] (Fig. 1a). In **1**, the malonate fills equatorial coordination positions of the Cu(II) ions, the rest of the positions being filled by water molecules. The magnetic properties of the bimetallic compounds (**1**) in the form $\chi_M T$ vs. T are shown in Fig. 1b and c, χ_M being the molar magnetic susceptibility per each Cu(II)M(II) couple. At room temperature, the values of $\chi_M T$ are 4.78(MnCu), 2.98(CoCu), 1.59(NiCu), 0.80(CuCu) and 0.40(ZnCu) $cm^3\ mol^{-1}\ K$, as expected for magnetically isolated $[Cu^{II}(mal)_2(H_2O)_2]^{2-}$ and $[M^{II}(H_2O)_6]^{2+}$ units. These values slightly decrease upon cooling down except for the complex CoCu where an abrupt decrease is observed. The magnetic behaviour of complexes MnCu, CoCu, NiCu, CuCu and ZnCu is typical of the coexistence of $[Cu^{II}(mal)_2(H_2O)_2]^{2-}$ and $[M^{II}(H_2O)_6]^{2+}$ units with very weak antiferromagnetic interactions mediated through hydrogen bonds, in agreement with their structure. Consequently, their magnetic properties were analysed through the Hamiltonian of Eq. (1) with the inclusion of a molecular field correction (θ) accounting for intramolecular interactions. In compound NiCu, the inclusion of an additional term accounting for the zero-field splitting (D) of the Ni(II) ion was considered (Eq. (2)):

$$\mathbf{H} = g_{Cu}\beta\mathbf{S}_{Cu}\boldsymbol{H} + g_M\beta\mathbf{S}_M\boldsymbol{H} \quad (1)$$

$$\mathbf{H} = g_{Cu}\beta\mathbf{S}_{Cu}\boldsymbol{H} + g_M\beta\mathbf{S}_M\boldsymbol{H} + \mathbf{S}_M D\mathbf{S}_M \quad (2)$$

Compound CuZn is the first one we analysed, the least-squares fitting to the experimental data through Eq. (1) leads to $g_{Cu} = 2.032(1)$, $\theta = -0.317(1)$ K and $R = 1.85 \times 10^{-5}$. Given that the geometry of the anion $[Cu^{II}(mal)_2(H_2O)_2]^{2-}$ remains practically constant for all the compounds, we keep the computed value of g_{Cu}

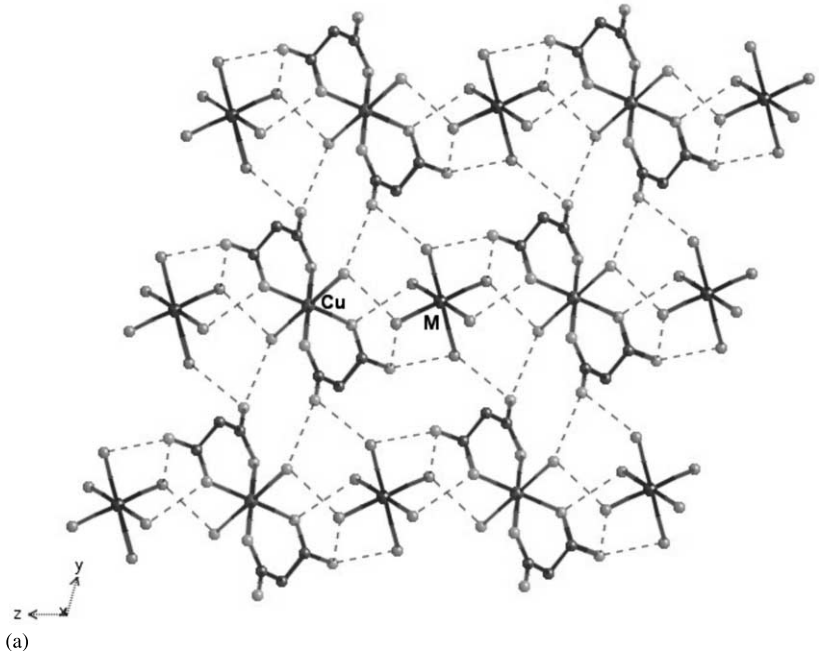

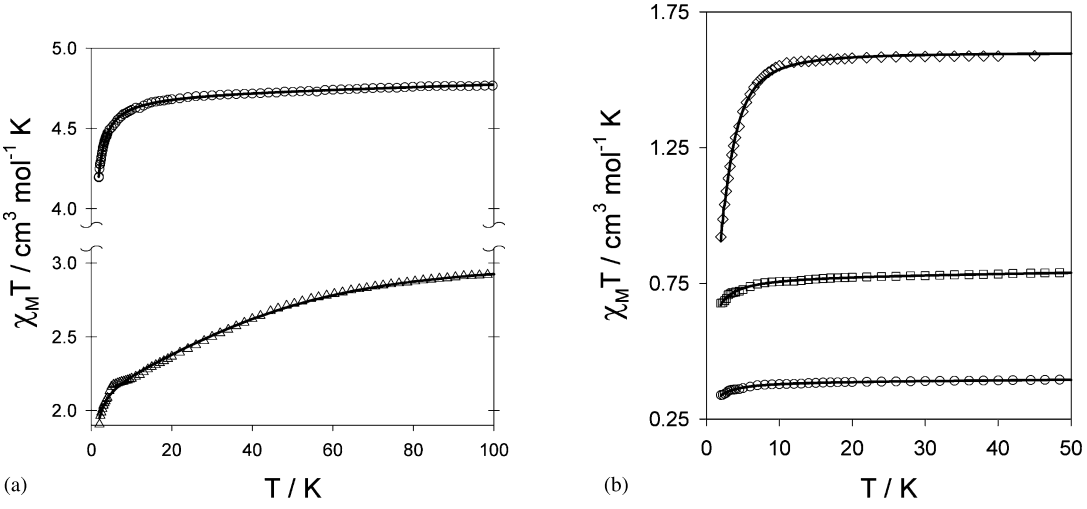

Fig. 1. (a) The 2D anion–cation network of hydrogen bonding in complex $[M^{II}(H_2O)_6][Cu^{II}(mal)_2(H_2O)_2]$ (M = Mn, Co, Ni, Cu and Zn). The six water molecules coordinated to M(II) ion act as space filling to join the neighbouring 2D layers of $[Cu(mal)_2(H_2O)_2]^{2-}$ forming a 3D hydrogen bonding network. (b) Thermal dependence of the $\chi_M T$ product (χ_M being the magnetic susceptibility per formula) for $[M^{II}(H_2O)_6][Cu^{II}(mal)_2(H_2O)_2]$ (M = Mn (○) and Co (△)). The solid lines are the best-fit curve through Eq. (1) (blue line for Mn) and through Eq. (3) (green line for Co). (c) Thermal dependence of the $\chi_M T$ product for the $[M^{II}(H_2O)_6][Cu^{II}(mal)_2(H_2O)_2]$ (M = Ni (◇), Cu (□) and Zn (○)). The solid lines are the best-fit curve through Eq. (1) (red line for Zn) and through Eq. (2) (black line for Ni).

for the remaining compounds. The best-fit parameters for complexes MnCu and CuCu are $g_M = 1.989(1)$ (MnCu) and 2.075(1) (CuCu), $\theta = 0.22(1)$ (MnCu) and $-0.47(1)$ (CuCu) K with $R = 1.21 \times 10^{-6}$ (MnCu) and 2.15×10^{-5} (CuCu). The best-fit parameters for CuNi are $g_{Ni} = 2.28(1)$, $\theta = -1.31(1)$ K and $R = 9.92 \times 10^{-4}$ and $g_{Ni} = 2.201(1)$, $|D| = 5.81(4)$ cm^{-1} and $R = 2.78 \times 10^{-5}$, respectively.

Concerning the magnetic behaviour of complex CoCu (Fig. 1b), once of the contribution of the $[Cu(mal)_2(H_2O)_2]^{2-}$ ion has been removed, the $\chi_M T$ values continuously decrease on lowering the temperature (values ranging from 2.42 cm^3 mol^{-1} K at room temperature to 1.42 cm^3 mol^{-1} K at 2 K). The mononuclear compounds containing a high-spin Co(II) ion in octahedral surrounding present magnetic properties deviating substantially from a Curie–Weiss law. There are several factors influencing the magnetic properties of the Co(II) in O_h symmetry such as the spin-orbit coupling (λ), the orbital reduction factor (κ), the axial crystal field splitting and the Figgis T_1-term mixing parameter. In a first approximation, we have considered

the Co(II) ion in a pure O_h symmetry, but all our attempts to fit the experimental data to that model failed, probably due to the distortion around the Co(II) octahedron. In a second approximation, only the two lowest Kramer doublets arising from the $^4A_2$ state are thermally populated. Then the energy separation (D) may be considered as a zero-field splitting within the quartet state, the Hamiltonian (Eq. (3)) to consider being then

$$\mathbf{H} = D(S_z^2 - \tfrac{5}{4}) + \beta \mathbf{S} g H \quad (3)$$

Under such approximation (and adding a field correction (θ) to the susceptibility, in order to take into account the intermolecular interactions), the fitting parameters are $\theta = -0.22$, $g_z = 2.49(1)$, $g_x = g_y = 2.30(1)$, $D = -52(1)$ cm^{-1} and $R = 1.55 \times 10^{-5}$. The theoretical curve matching very well the experimental data in all temperature range (see Fig. 1b).

Some ligands can bridge the metallic ions, but if the malonate is kept as bidentate the molecules remain isolated as in $[Cu_2(mal)_2(H_2O)_2(bipym)]$ [15], here the dimensionality and the magnetic coupling being governed by the complementary ligand.

2.2. η^5-Bidentate + unidentate

In this coordination, mode two of the oxygens coordinate the same metal and another one is bound to an additional metal as unidentate, the ligand behaving overall as tridentate. The remaining oxygen acts as acceptor in hydrogen bonding blocking the polymerisation in this direction.

The simplest compound exhibiting this coordination mode is the $[(H_2O)_4Cu(\mu\text{-mal})Cu(mal)(H_2O)_2]$ dimer (**2**) [9,18] (Fig. 2a), in which Cu(1) and Cu(2) are in octahedral and square-pyramidal environments, respectively. The malonate-oxygens fill equatorial positions at Cu(1), the Cu(1)–O distances being shorter, whereas the Cu(2)–O distance is long, the malonate oxygen filling an apical position with respect to Cu(2). We have observe in this compound the copper(II) ions to be ferromagnetically coupled. The magnetic coupling constant having a value of $J = 1.8$ cm^{-1} (Fig. 2b). We can find in the literature that 95% of copper(II) dimers exhibit an antiferromagnetic coupling, but as we will see in our compounds the ferromagnetic behaviour is much more frequent than the antiferromagnetic one.

In square-pyramidal and octahedral environments, the magnetic orbital at each copper(II) atom is defined by the short equatorial (or basal) bonds, and it is of the $d_{x^2-y^2}$ type with possible some mixture of the d_{z^2} character in the axial position. In **2**, the carboxylate couples a $d_{x^2-y^2}$ magnetic orbital of Cu(1) with a d_{z^2} of Cu(2), the latter being not-magnetic and orthogonal to its magnetic $d_{x^2-y^2}$. This kind of coupling (basal-apical or equatorial-axial) is repeated in many compounds and it has been found to be ferromagnetic in all of our copper(II) compounds.

The trinuclear cation $[Cu_3(mal)_2(H_2O)_9]^{2+}$ (Fig. 2a) present in $\{[Cu(H_2O)_4]_2[Cu(mal)_2(H_2O)]\}$ $[Cu(mal)_2(H_2O)_2]\{[Cu(H_2O)_4][Cu(mal)_2(H_2O)_2]\}$ (**3**) [9] is formed by a central aquabis(malonate)copper(II) entity that is linked to two peripheral tetraaquacopper(II) units through carboxylato bridges which exhibit the *anti–syn* configuration. The coordination around the two crystallographically independent copper atoms (Cu(3) and Cu(4)) is distorted square-pyramidal. Four coplanar carboxylate oxygen atoms from two malonate ligands with nearly identical bond lengths (1.938(4) and 1.941(2) Å for Cu(3)–O(9) and Cu(3)–O(10), respectively) build the basal plane around Cu(3), whereas a weakly coordinated water molecule (2.508(3) Å for Cu(3)–O(7w)) occupies the axial position. At Cu(4), four water molecules build the basal plane and a malonate-oxygen occupies the axial position. The magnetic behaviour is shown in Fig. 2c. The copper(II) ions being ferromagnetically coupled ($J = 1.2$ cm^{-1}) by the same reasons as previously mentioned for **2**.

The compound $\{[Cu(H_2O)_3][Cu(mal)_2(H_2O)]\}_n$ (**4**) [9] (Fig. 3a) has a 1D polymeric structure. It consists of zigzag chains of copper(II) ions that exhibit a regular alternation of aquabis(malonate)copper(II) and triaquocopper(II) units, the former being linked to the latter as bis-monodentate ligands though two *trans*-malonate oxygen atoms. The chains run parallel to the z-axis, and they are interconnected trough hydrogen bonding. The two crystallographically independent copper(II) ions (Cu(1) and Cu(2)) have distorted square-pyramidal surroundings. The four coplanar carboxylate oxygen atoms (O(1), O(3), O(5), and O(6)), which are coordinated to Cu(1) define the basal plane, whereas the apical positions is occupied by a weakly coordinated water molecule O(1w). The three water molecules O(2w), O(3w) and O(4w) and the carboxylate oxygen O(7) build the basal plane at Cu(2), whereas the other carboxylate oxygen, O(2c) ($c = -x, \frac{1}{2} - y, -\frac{1}{2} + z$), occupies the axial position.

Each malonate simultaneously adopts bidentate (at Cu(1)) and unidentate (at Cu(2)) coordination modes. Two slightly different carboxylate bridges, that exhibit the *anti–syn* conformation, alternate regularly within each copper(II) chain.

For this compound, the magnetic behaviour is shown in Fig. 3b. The O(1)–C(1)–O(2) carboxylate connects a basal Cu(1)–O(1) bond with an apical O(2)–Cu(2b) bond; this coupling being weak and ferromagnetic ($J = 1.9$ cm^{-1}) as observed in **2**. The O(5)–C(5)–O(5) carboxylate connects two equatorial bonds (Cu(1)–O(5) and Cu(2)–O(7)) but the carboxylato plane and the equatorial plane at Cu(2) (O(2w)O(4w)O(3w)O(7))

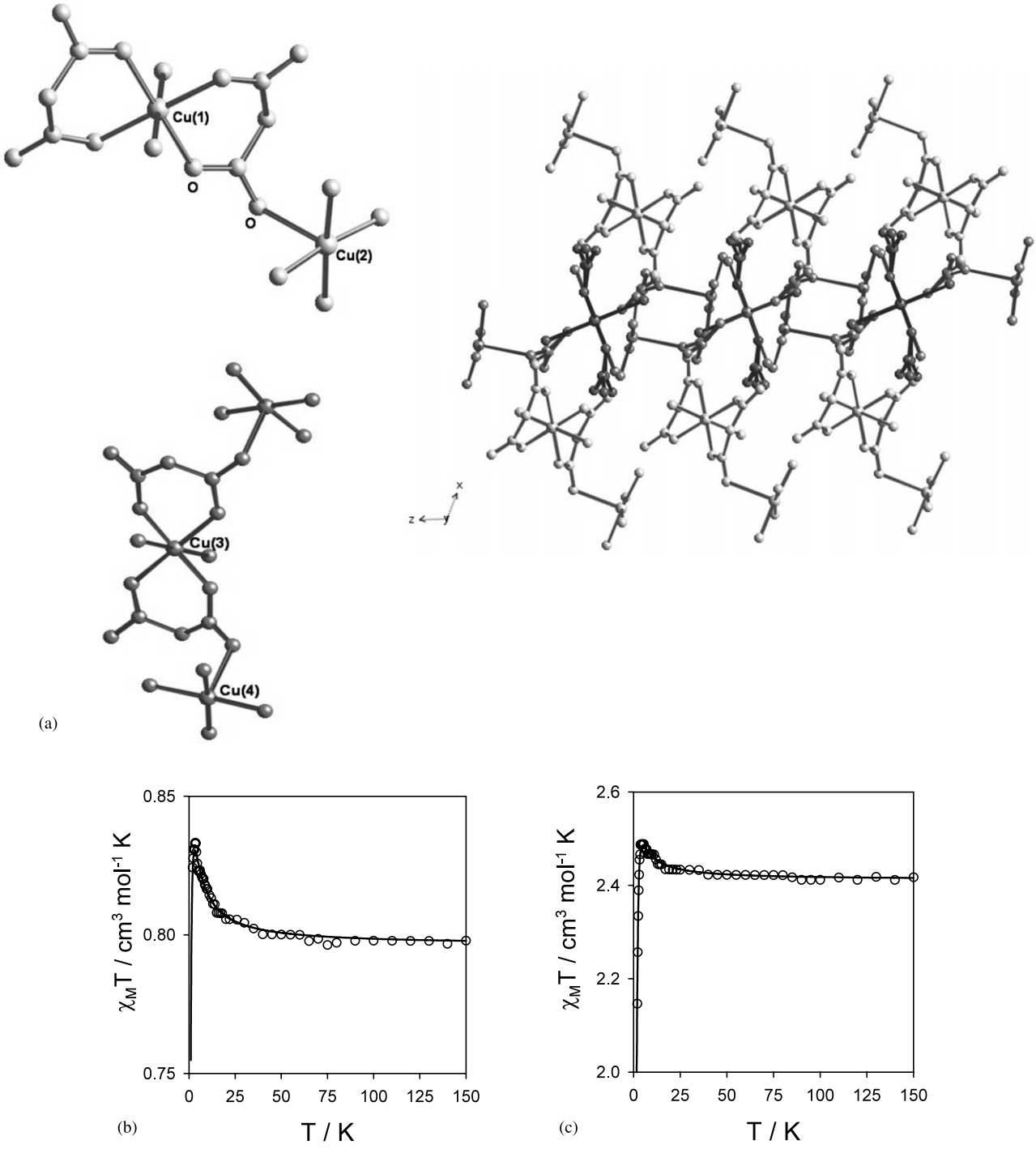

Fig. 2. (a) Perspective view of the trinuclear copper(II) units of compound $\{[Cu(H_2O)_4]_2[Cu(mal)_2(H_2O)]\}[Cu(mal)_2(H_2O)_2]$-$\{[Cu(H_2O)_4][Cu(mal)_2(H_2O)_2]\}$ along the b-axis. Contents of the unit cell of the complex: monomer (violet), dimer (green) and trimer (orange). (b) Thermal dependence of the $\chi_M T$ product for compound $[(H_2O)_4Cu(\mu\text{-mal})Cu(mal)(H_2O)_2]$ (**2**) (dimer). Solid line is the best-fit by the appropriate expression through the Hamiltonian $\mathbf{H} = -J\mathbf{S}_A\mathbf{S}_B + g\beta(\mathbf{S}_A + \mathbf{S}_B)H + \mathbf{S}_A D\mathbf{S}_B$. (c) Thermal dependence of the $\chi_M T$ product for compound $\{[Cu(H_2O)_4]_2[Cu(mal)_2(H_2O)]\}$ $[Cu(mal)_2(H_2O)_2]$ $\{[Cu(H_2O)_4][Cu(mal)_2(H_2O)_2]\}$(**3**). Solid line is the best-fit derived through the Hamiltonian $\mathbf{H} = -J(\mathbf{S}_{Cu3}\mathbf{S}_{Cu4} + \mathbf{S}_{Cu3}\mathbf{S}_{Cu4\alpha}) + \Sigma_{i=1}^{3} g_{Cu_i}\beta\mathbf{S}_{Cu_i}H$.

are nearly orthogonal (dihedral angle of 94.4°), this may explain this interaction to be ferromagnetic ($J = 3.0$ cm^{-1}).

Combining the malonate with blocking ligands, such as imidazole or methylimidazole, 1D polymeric structures can be obtained as those observed in compounds $[Cu(Im)_2(mal)]$ (**5**) and $[Cu(MeIm)_2(mal)]$ (**6**) [19] (Fig. 4a and b). In these compounds, copper(II) is in a square-pyramidal surrounding. Two malonate-oxygens from a bidentate malonate and two imidazole-nitrogens build

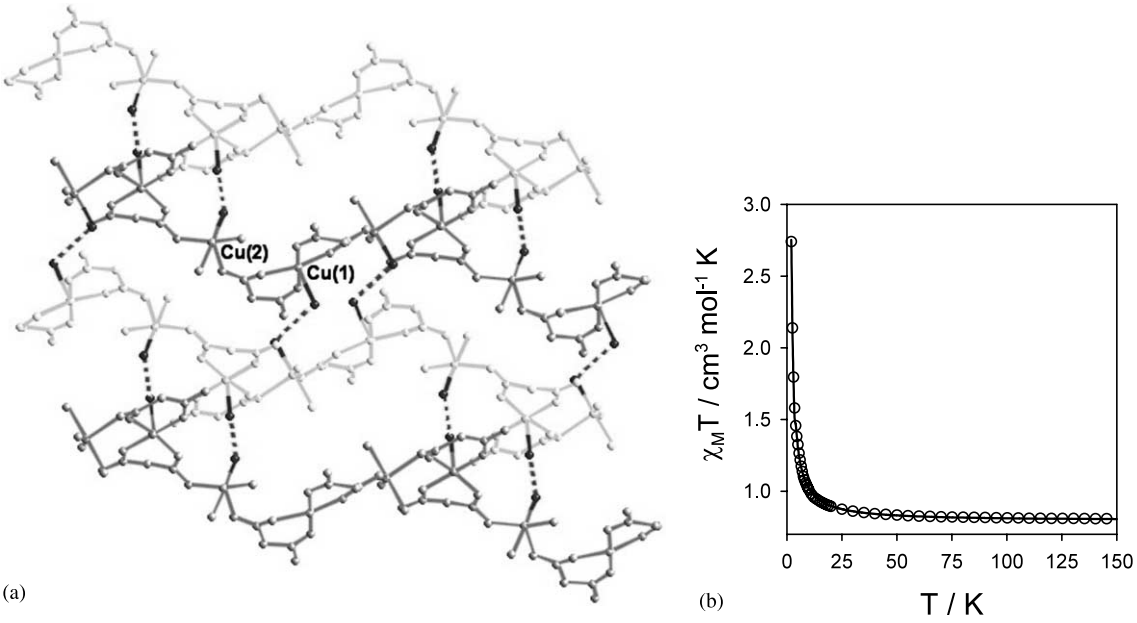

Fig. 3. (a) Projection of the structure of **4** down the *a*-axis, showing the sheet-like nature. (b) Thermal dependence of the $\chi_M T$ product for compound $\{[Cu(H_2O)_3][Cu(mal)_2)(H_2O)]\}_n$ (**4**). Solid line is the best-fit derived through the Hamiltonian $\mathbf{H} = -J\Sigma_i[\mathbf{S}_{2i}\mathbf{S}_{2i-1} + \alpha\mathbf{S}_{2i}\mathbf{S}_{2i+1}]$.

the basal plane. The same malonate ligand acts as unidentate towards the neighbouring copper(II) filling an apical position with a longer Cu–O distance. The magnetic behaviour is shown in Fig. 4c, both compounds exhibit ferromagnetic coupling, $J = 1.64(1)$ and $J = 0.39(1)$ cm^{-1} for **5** and **6**, respectively, as expected from the apical-equatorial connection.

With 2,4′-bipyridine, a tetrameric neutral unit $[Cu_4(mal)_4(H_2O)_4(2,4'\text{-bipy})_4]$ (**7**) can be obtained, involving a small planar-square with copper(II) cations and malonate anions at each corner [20] (Fig. 5a and b). Each copper atom exhibits a slightly distorted square-pyramidal surrounding. The 2,4′-bipy acts as blocking ligand, since the location of the nitrogen in 2 does not allow further polymerisation. The magnetic properties of **7** are shown in Fig. 6 and correspond to those of magnetically isolated squares of four ferromagnetically coupled spin doublets, $J = 12.3(1)$ cm^{-1}. The magnetic properties of **7** under the form of $\chi_M T$ plot are shown in Fig. 6. The $\chi_M T$ plot for **7** continuously increases as the temperature is lowered reaching a plateau at 3.0 K ($\chi_M T = 3.24$ cm^3 mol^{-1} K) which is as expected for a magnetically isolated square of four spin doublets interacting ferromagnetically (low-lying $S = 2$ accounting for the plateau observed for $\chi_M T$).

$[Cu_4(mal)_4(H_2O)_4(4,4'\text{-bipy})_2]\cdot 2H_2O$ (**8**) has similar structure and magnetic properties to those observed for **7**. The main difference is the ability of the 4,4′-bipy to act as bidentate ligand interconnecting the $Cu_4(mal)_4(H_2O)_4$ tetramers leading to a 2D network [21] (Fig. 7). This compound illustrates the increment of the dimensionality by the introduction of other bridging ligands. The four copper(II) ions are ferromagnetically coupled in the small square ($J = 12.4(1)$ cm^{-1}) existing weak antiferromagnetic interactions among the tetramers trough the 4,4′-bipy ($J = -0.05$ cm^{-1}) (see Fig. 6). For compound **8**, $\chi_M T$ continuously increases reaching a maximum of 2.93 cm^3 mol^{-1} K at 5.5 K and further decreases at lower temperatures (see Fig. 6). The magnetic behaviour of **8** is satisfactorily interpreted considering a quadratic layer of ferromagnetically coupled tetranuclear copper(II) units, which are antiferromagnetically coupled through the bridging 4,4′-bpy. The magnetic coupling within the tetramer is strong and ferromagnetic ($J = 12.4$ cm^{-1}), whereas the coupling through the bridging 4,4′-bpy is antiferromagnetic and very weak ($J_{eff} = -0.052$ cm^{-1}).

Also we obtained heterometallic structures, e.g., $[Mn^{II}Cu^{II}(mal)_2(H_2O)_3]\cdot 2H_2O$ (**9**) [22], made up by neutral bimetallic chains that linked with long weak axial malonate oxygen to copper bonds, which leads to a corrugated sheet-like structure (Fig. 8a). The magnetic behaviour, shown in Fig. 8b, is characteristic of ferrimagnetic chains without magnetic ordering in the temperature range explored. Given the special alternating trend $\ldots J_1\text{–}J_1\text{–}J_2\text{–}J_2\text{–}J_1\text{–}J_1\ldots$ where J_1 and J_2 represent the intrachain Cu(II)–Mn(II) isotropic magnetic coupling and the lack of a theoretical model to treat it, we have assumed that the J_1 and J_2 values should be very close and consequently, we have treated the experimental data through a regular chain approach. The least-square fitting of the data led to $J_{MnCu} = -4.5$ cm^{-1} [11].

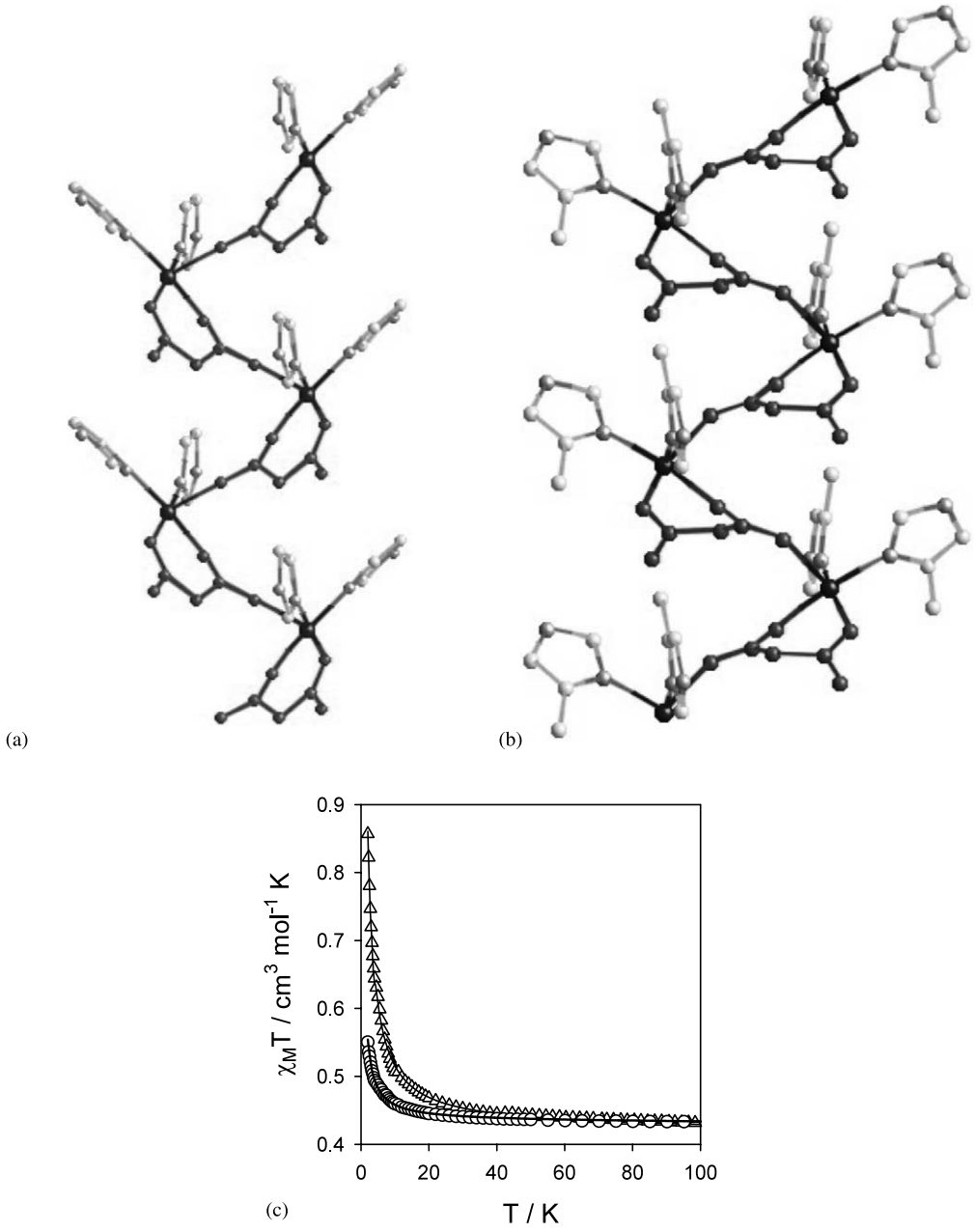

Fig. 4. (a) Projection of compound $[Cu(Im)_2(mal)]$ (**5**) down the *a*-axis showing the parallel arrangement of the chains. (b) Projection of compound $[Cu(MeIm)_2(mal)]$ (**6**) down the *b*-axis. (c) Thermal dependence of the $\chi_M T$ product for compounds $[Cu(Im)_2(mal)]$ (△) and $[Cu(MeIm)_2(mal)]$ (○). Solid lines are the best-fit through the magnetic susceptibility expression derived from the Hamiltonian $\mathbf{H} = -J\Sigma_i \mathbf{S}_i \mathbf{S}_{i+1}$.

2.3. *Bidentate + bis(unidentate)*

Two polymorphic malonate-bridged copper(II) complexes of formula $\{[Cu(bpy)(H_2O)][Cu(bpy)(mal)(H_2O)]\}(ClO_4)_2$ (**10**) (Fig. 9) have been prepared [8]. The structures are made up of uncoordinated perchlorate anions and malonate-bridged zigzag copper(II) chains running parallel to one of the crystallographic axes. These chains are built by a $[Cu(bpy)(mal)(H_2O)]$ unit acting as bis-unidentate ligand toward two $[Cu(bpy)(H_2O)]$ adjacent units trough its OCCCO skeleton in an *anti–anti* conformation, whereas the carboxylate bridge exhibits the *anti–syn* conformation. These compounds contain four crystallographically independent copper(II) atoms, but the environment of all of them is distorted square-pyramidal: the axial position is occupied by a water molecule, whereas the equatorial plane is formed by a chelating bpy and either a bidentate malonate or two unidentate carboxylate-oxygens from two malonate ligands. Each malonate acts as bidentate respect to a copper(II) and as bis(unidentate) to other two. The analysis of the magnetic data indicates the

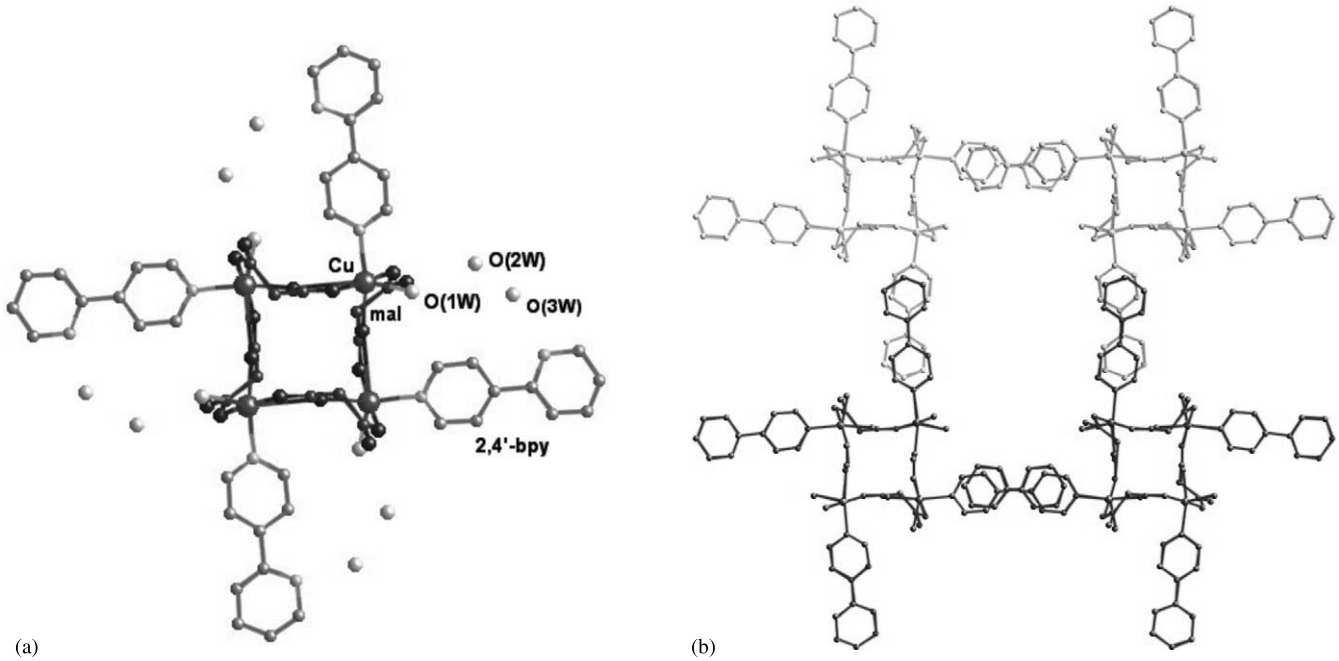

Fig. 5. (a) Perspective view of the tetramer unit of $[Cu_4(mal)_4(H_2O)_4(2,4'\text{-bipy})_4]\cdot 2H_2O$ (**7**). (b) Perspective view of the stacking of the compound along the *c*-axis.

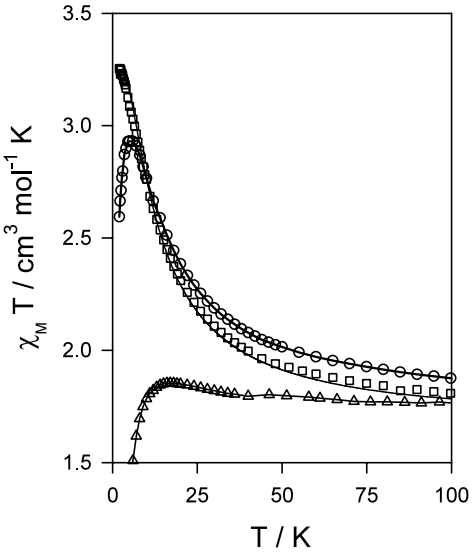

Fig. 6. Thermal dependence of the $\chi_M T$ product for compounds (**7**) $[Cu_4(mal)_4(H_2O)_4(2,4'\text{-bipy})_4]\cdot 2H_2O$ (□), (**8**) $[Cu_4(mal)_4(H_2O)_4(4,4'\text{-bipy})_2]\cdot 2H_2O$ (○) and (**15**) $[Cu_4(mal)_4(pyz)_2]\cdot 4H_2O$ (△), χ_M being the magnetic susceptibility per four copper(II) ions. Solid lines are the best-fit by the Hamiltonian $\mathbf{H} = -J(\mathbf{S}_1\mathbf{S}_2 + \mathbf{S}_2\mathbf{S}_3 + \mathbf{S}_3\mathbf{S}_4 + \mathbf{S}_1\mathbf{S}_4)$.

occurrence of a ferro- (through the carboxylate, $J = 4.6$ cm^{-1}) and antiferromagnetic (through the skeleton of the malonate, $J = -4.2$ cm^{-1}) coupling.

A family of compounds exhibiting this coordination mode are the isostructural [23,24] homo or hetero-bimetallic malonates of the divalent Co, Ni and Zn: $[M(H_2O)_2][M'(mal)_2(H_2O)_2]$ ($M = Mn^{II}$, Co^{II}, Ni^{II}, Zn^{II}; $M' = Co^{II}$, Ni^{II}, Zn^{II}) (**11**) (Fig. 10a and b). The simple malonates of the divalent Co, Ni and Zn are isostructural, and their mixed bimetallic malonates behave as solid solutions filling randomly the positions of M and M′. Mn(II) can also be introduced in the network as M, its concentration must be kept below 50% or the mixed malonate is impurified with Mn(II) malonate remaining malonate-oxygens act as unidentate filling equatorial positions of four adjacent M cations. The magnetic coupling, shown for the Ni(II) complex in Fig. 10c, is very weak since the malonate exhibits the *anti–syn* configuration, being ferromagnetic and antiferromagnetic for Ni(II) and Co(II), respectively. The mixed malonates are ferrimagnetic, but magnetic ordering is not obtained in any case.

The structure of the Mn(II) malonate (**12**) is made up by the polymerisation of $[Mn(mal)(H_2O)_2]$ monomers giving a 2D array (Fig. 11a and b) [25]. Mn(II) is in an octahedral environment, with the water molecules in the axial positions. Each malonate chelates the metal as bidentate, with the remaining two oxygens bridging to two further adjacent metallic atoms as bis-unidentate. This structure is very original since the two carboxylates of the malonate exhibit two different conformations, the *anti–anti* and the *anti–syn*, respectively. This feature leads to a spin canting behaviour at low temperatures (Fig. 11c).

$[M(mal)(pyz)(H_2O)]$, $[M(mal)(pym)(H_2O)]$ (M(II) = Co, Zn) (**13**) [26], and $[Co(mal)(4,4'\text{-bipy})_{1/2}(H_2O)]$ [21] $[Mn(mal)(4,4'\text{-bipy})_{1/2}(H_2O)]$ (**14**) [24] have related structures in which layers of octahedrally coordinated metallic atoms bridged by the malonate anions within the layers are interconnected by 4,4′-bipy, pyz or pym molecules leading to a 3D structure. Each malonate

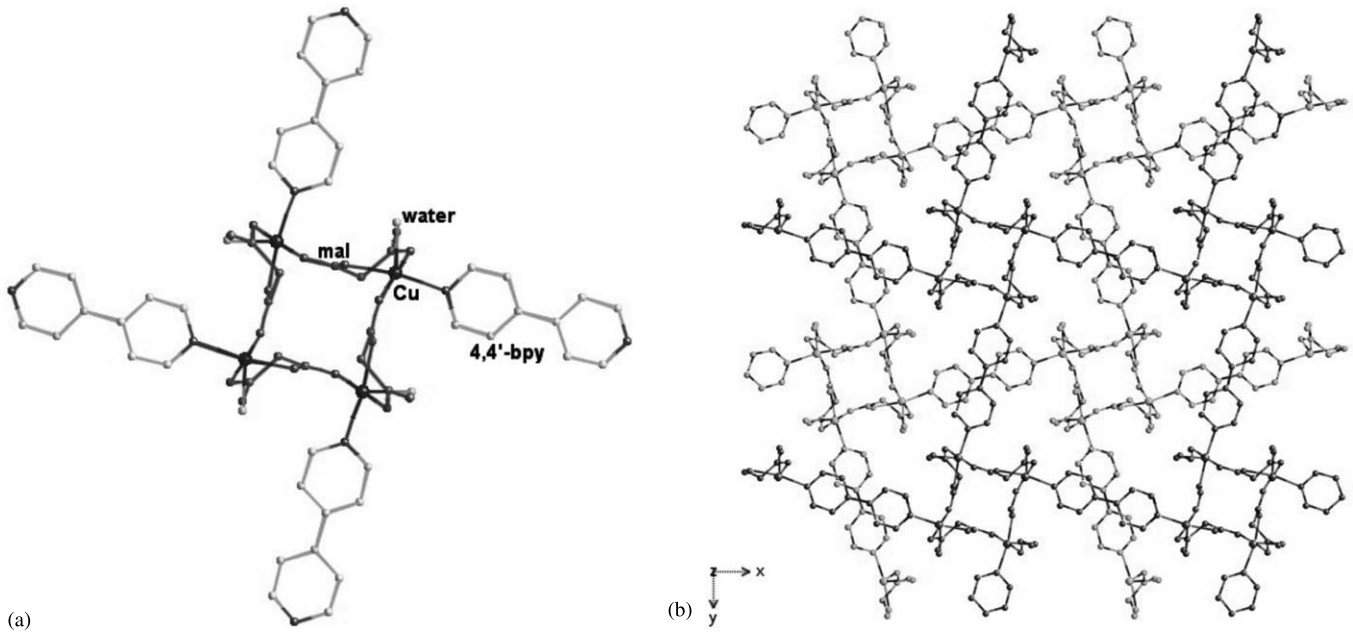

Fig. 7. (a) Perspective view of the tetramer unit of $[Cu_4(mal)_4(H_2O)_4(4,4'\text{-bipy})_2]\cdot 2H_2O$ (**8**) along the *c*-axis when only the odd layers are considered. (b) View of the layers stacked along the tetragonal *c*-axis.

chelates the metal as bidentate, with the remaining two oxygen atoms bridging to two further adjacent metallic atoms as bis-unidentate, thus forming continuous covalently bonded sheets. The metal is then coordinated by three different malonate anions, the remaining two *trans*-positions being filled by a terminal H_2O molecule and the nitrogen of the aromatic molecule. All these compounds, except those of Zn, exhibit weak antiferromagnetic coupling.

The structure of $[Cu_4(mal)_4(pyz)_2]\cdot 4H_2O$ (**15**) [20] (Fig. 12) is very similar to that of **8**, in which 2D layers were obtained by the assemblage of $Cu_4(mal)_4$ tetramers by bidentate 4,4′-bipy ligands. In **15**, the tetramers are assembled by bidentate pyrazine ligands. Each copper atom is in a quasi-perfect square-pyramidal surrounding with three carboxylate-oxygen atoms from two malo-

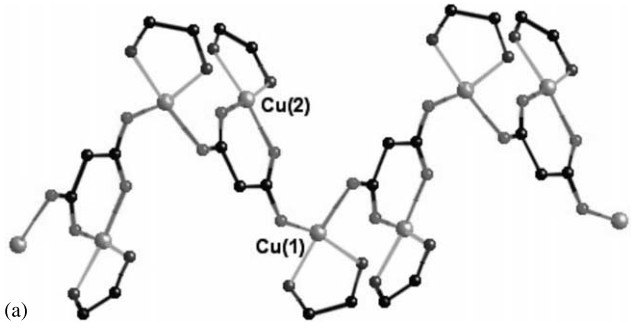

Fig. 9. View of compound $\{[Cu(bpy)(H_2O)][Cu(bpy)(mal)(H_2O)]\}(ClO_4)_2$ (**10**) showing the parallel arrangement of the chains along the *b*-axis. 2,2′-Bipyridine ligands, water molecules and the perchlorate anions have been omitted for clarity.

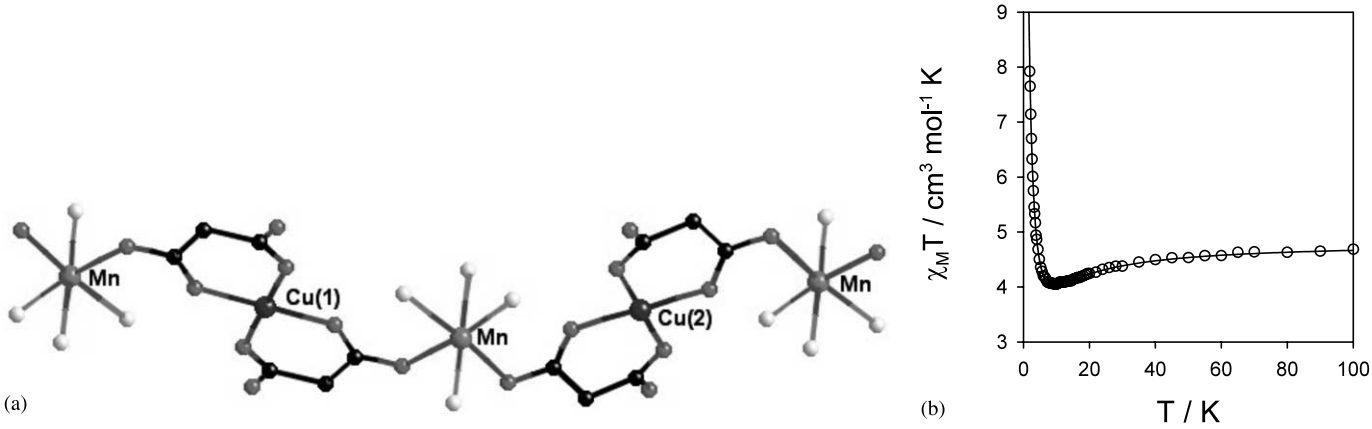

Fig. 8. (a) Perspective drawing of a fragment of the chain of $[Mn^{II}Cu^{II}(mal)_2(H_2O)_3]\cdot 2H_2O$ (**9**). (b) Thermal dependence of the $\chi_M T$ product for compound **9**.

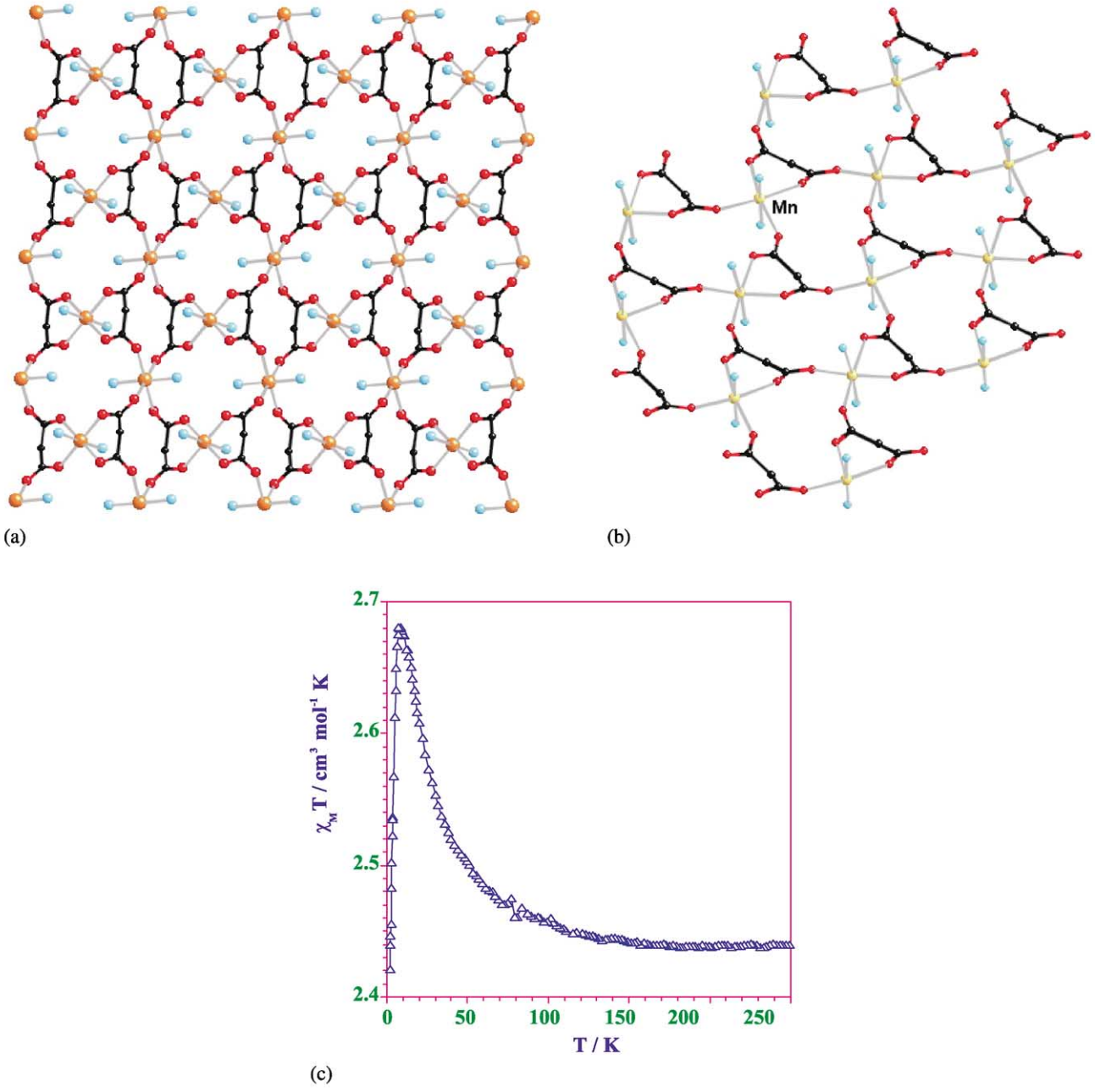

Fig. 10. (a) Layer of $[M(H_2O)_2][M'(mal)_2(H_2O)_2]$ ($M = Co^{II}$, Ni^{II}, Zn^{II}; $M' = Co^{II}$, Ni^{II}, Zn^{II}) (**11**). (b) Sheet structure of compound $[Mn(mal)(H_2O)_2]$ (**12**). (c) Thermal dependence of the $\chi_M T$ product for $[Ni(H_2O)_2][Ni(mal)_2(H_2O)_2]$.

nate groups and one nitrogen atom from a pyrazine ligand building the equatorial plane. The main difference with the structure of **8** is the absence of a water molecule filling the apical position of the square-pyramidal surrounded copper(II). This position is occupied by a malonate-oxygen of a tetramer of a neighbouring layer. By this new link, the layers are interconnected leading to a 3D structure. Each malonate uses its four oxygen atoms to coordinate the copper atoms: within each layer, the malonate adopts simultaneously the bidentate (at one copper atom) and unidentate (at another copper atom) coordination modes, the fourth carboxylate-oxygen acts also as unidentate being bound to a further copper atom from a neighbouring layer. The magnetic properties of **15** have been investigated in the temperature range 1.9–300 K and they look like an overall weak ferromagnetic behaviour which would be the result of a competition between ferro- (through the malonate bridge) and antiferromagnetic (through the pyrazine bridge) interactions, the former being somewhat stronger are consistent with the occurrence of a competition between a ferromagnetic

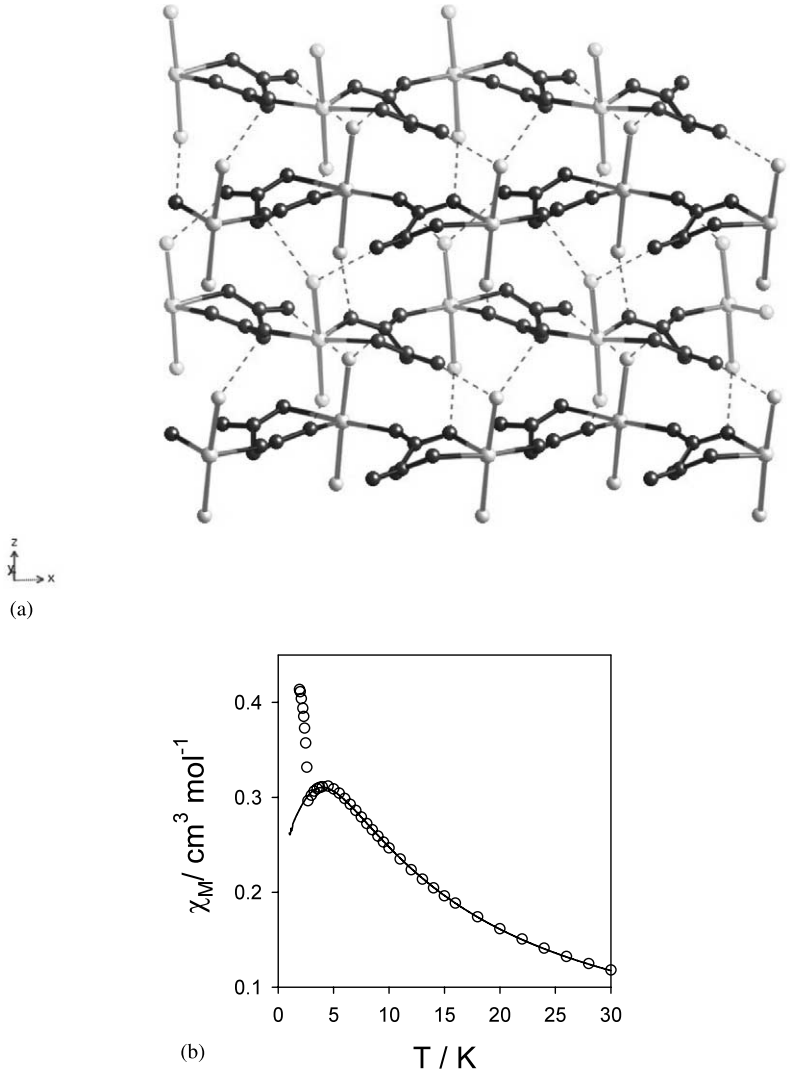

Fig. 11. (a) Parallel packing of the sheets showing the hydrogen interactions involved in the generation of the framework structure in compound **12**. (b) Thermal dependence of the χ_M for [Mn(mal)(H_2O)$_2$]. Solid line is best-fit through the Hamiltonian $\mathbf{H} = -J\Sigma_i \mathbf{S}_i \mathbf{S}_{i+1}$.

coupling through the malonate bridge and an antiferromagnetic one through the pyrazine bridge. However, there is no long-range antiferromagnetic ordering in the temperature range studied (Fig. 6).

3. Conclusions

The bis-bidentate coordination mode dominant in the oxalato complexes is sterically forbidden for the malonate, this makes the bidentate + unidentate and the bidentate + bis-unidentate coordination modes to dominate in the chemistry of the malonate. This affects dramatically to the structure and the properties of the malonate complexes, being the ferromagnetic interactions much more frequent than in general compounds. The malonate is a dissymmetric ligand. By its bidentate side, it is a strong complexing agent (due to the chelate effect) and it will be usually filling equatorial or basal positions displaying short M–O distances. By its other side it acts as unidentate showing weaker interactions and longer M′–O distances. The metallic ion that is chelated usually remains in the same plane of the carboxylato groups with small deviations; on the other hand, the unidentate coordinated metal can deviate considerably from the carboxylate plane, reducing notably the overlap between the magnetic orbitals of the paramagnetic centres. This minimises the antiferromagnetism and interactions expected to be antiferromagnetic can be turned to ferromagnetic. Another feature of the malonate is the fact that when these latter M′–O distances are long enough, this oxygen becomes axial or apical. Then, as a consequence of the coupling of orbitals of different symmetry, the magnetic interaction is expected to be ferromagnetic in many copper(II) complexes.

Consequently, we can conclude that the malonate is a very versatile ligand that is able to generate high

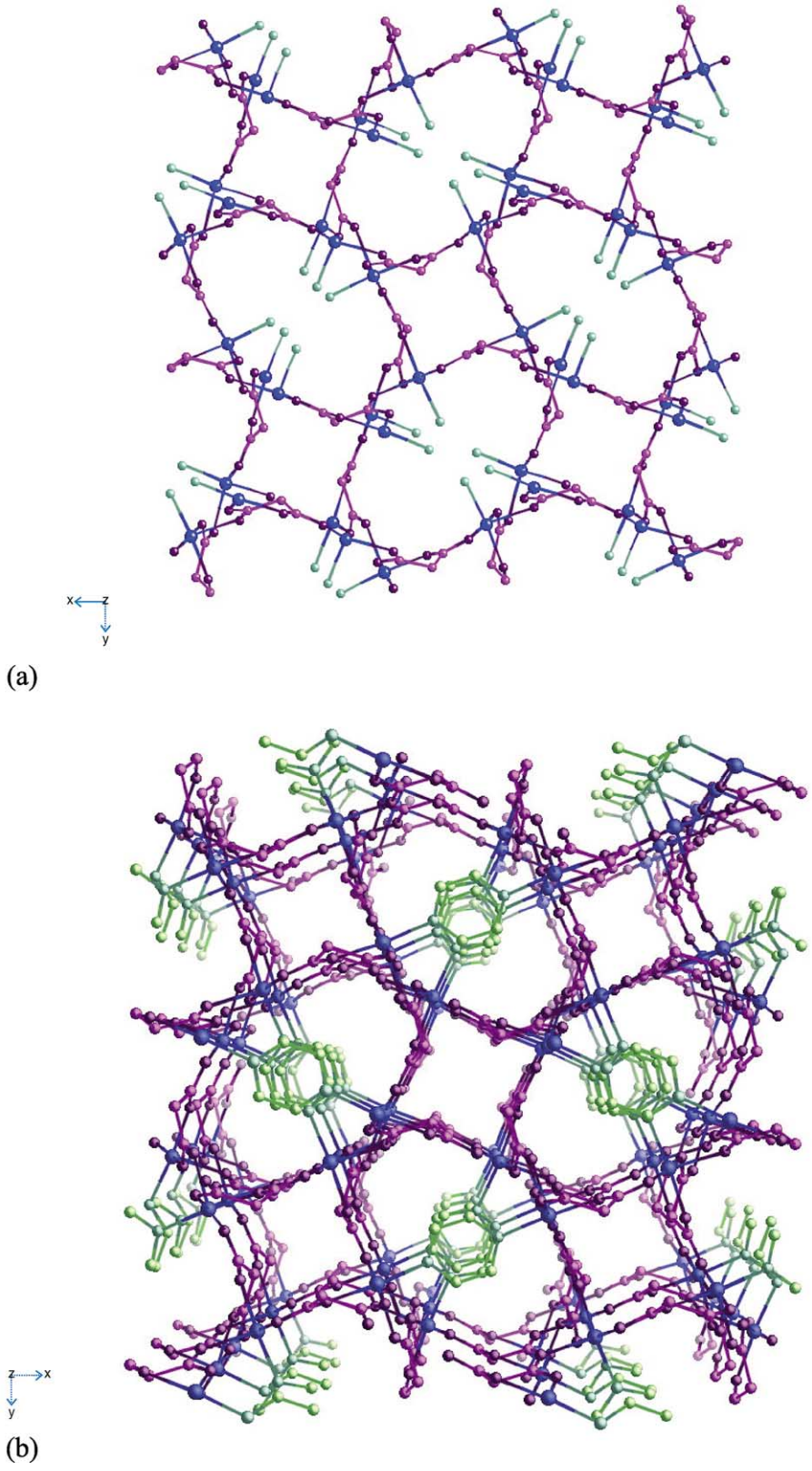

Fig. 12. (a) The Cu/malonate framework in compound $[Cu_4(mal)_4(pyz)_2]\cdot 4H_2O$ (**15**) along the *c*-axis. (b) A view of the 3D structure where the square grids layers are stacked along the *c*-axis showing the π–π overlap between pairs of pyrazine molecules.

dimensionality networks coupling paramagnetic centres ferromagnetically in much higher percentage than other dicarboxylic ligands. The malonate itself cannot lead to a 3D array, but combined with other ligands the 3D networks can be obtained. We are now in the search of ligands, suitable to be combined with the malonate, capable to couple ferromagnetically the spin carriers in the remaining dimensions.

Acknowledgements

The financial support provided by the Gobierno Autónomo de Canarias (Project PI2002/175) and the Spanish Dirección General de Investigación (Ministerio de Ciencia y Tecnología), through project BQU2001-3794, is gratefully acknowledged. J.P. thanks Ministerio de Educación y Cultura for a Predoctoral-fellowship AP2001-3322 and F.S.D. thanks the Consejería de Educación, Cultura y Deportes (Gobierno Autónomo de Canarias) for a predoctoral fellowship.

References

[1] D. Gatteschi, O. Kahn, J.S. Miller, F. Palacio, Magnetic Molecular Materials, Kluwer Academic Publishers, Dordrecht, The Netherlands, 1991.
[2] H. Iwamura, K. Itoh, M. Kinoshita, Proceedings of the International Symposium on Chemistry and Physics of Molecular-based Magnetic Materials, Molecular Crystals and Liquid Crystals, Gordon & Breach, London, 1993.
[3] J.S. Miller, A.J. Epstein, Proceedings of the IV International Conference on Molecule-based Magnets, Molecular Crystals and Liquid Crystals, Gordon & Breach, London, 1995.
[4] D. Chattopadhyay, S.K. Chattopadhyay, P.R. Lowe, C.H. Schwalke, S.K. Mazumber, A. Rana, S. Ghosh, J. Chem. Soc., Dalton Trans. (1993) 913.
[5] I. Gil de Muro, F.A. Mautner, M. Insausti, L. Lezama, M.I. Arriortua, T. Rojo, Inorg. Chem. 37 (1998) 3243.
[6] C. Ruiz-Pérez, J. Sanchiz, M. Hernández-Molina, F. Lloret, M. Julve, Inorg. Chim. Acta 298 (2000) 202.
[7] E. Suresh, M.H. Bhadbhade, Acta Crystallogr. C 53 (1997) 193.
[8] C. Ruiz-Pérez, M. Hernández-Molina, P. Lorenzo-Luis, F. Lloret, J. Cano, M. Julve, Inorg. Chem. 39 (2000) 3845.
[9] C. Ruiz-Pérez, J. Sanchiz, M. Hernández-Molina, F. Lloret, M. Julve, Inorg. Chem. 39 (2000) 1363.
[10] C. Oldham, in: G. Wilkinson, R.D. Gillard, J.A. McCleverty (Eds.), Comprehensive Coordination Chemistry, vol. 2, Pergamon Press, Oxford, 1987, p. 435.
[11] D.K. Towle, S.K. Hoffmann, W.E. Hatfield, P. Singh, P. Chaudhuri, Inorg. Chem. 27 (1988) 394.
[12] P.R. Levstein, R. Calvo, Inorg. Chem. 29 (1990) 1581.
[13] F. Sapiña, E. Escrivá, J.V. Folgado, A. Beltrán, A. Fuertes, M. Drillon, Inorg. Chem. 31 (1992) 3851.
[14] (a) E. Colacio, J.P. Costes, R. Kivekäs, J.P. Laurent, J. Ruiz, Inorg. Chem. 29 (1990) 4240;
(b) E. Colacio, J.M. Domínguez-Vera, J.P. Costes, R. Kivekäs, J.P. Laurent, J. Ruiz, M. Sundberg, Inorg. Chem. 31 (1992) 774;
(c) E. Ruiz, Inorg. Chem. 212 (1993) 115.
[15] Y. Rodríguez-Martín, J. Sanchiz, C. Ruiz-Pérez, F. Lloret, M. Julve, Inorg. Chim. Acta 326 (2001) 20.
[16] W.-L. Kwik, K.-P. Ang, H.S.-O. Chan, J. Chem. Soc., Dalton Trans. (1986) 2519.
[17] (a) Y. Rodríguez-Martín, J. Sanchiz, C. Ruiz-Pérez, F. Lloret, M. Julve, Cryst. Eng. Commun. 4 (2002) 631;
(b) G.I. Bimitrova, A.V. Ablov, G.A. Kiosse, G.A. Popovich, T.I. Nmalinouskii, I.F. Bourshteyn, Dokl. Akad. Nauk SSSR 216 (1974) 1055.
[18] D. Chattopadhyay, S.K. Chattopadhyay, P.R. Lowe, C.H. Schwalde, S.K. Mazumder, A. Rana, S. Ghosh, J. Chem. Soc., Dalton Trans. (1993) 913.
[19] J. Sanchiz, Y. Rodríguez-Martín, C. Ruiz-Pérez, A. Mederos, F. Lloret, M. Julve, New J. Chem. 26 (2002) 1624.
[20] Y. Rodríguez-Martín, M. Hernández-Molina, F.S. Delgado, J. Pasán, C. Ruiz-Pérez, J. Sanchiz, F. Lloret, M. Julve, Cryst. Eng. Commun. 4 (2002) 1.
[21] Y. Rodríguez-Martín, C. Ruiz-Pérez, J. Sanchiz, F. Lloret, M. Julve, Inorg. Chim. Acta 318 (2001) 159.
[22] C. Ruiz-Pérez, J. Sanchiz, M. Hernández-Molina, F. Lloret, M. Julve, Inorg. Chim. Acta 298 (2000) 202.
[23] C. Ruiz-Pérez, Y. Rodríguez-Martín, J. Sanchiz, M. Hernández-Molina, F.S. Delgado, J. Pasán, F. Lloret, M. Julve, Eur. J. Inorg. Chem., submitted for publication.
[24] N.J. Ray, B.J. Hathaway, Acta Crystallogr. B 38 (1982) 770.
[25] T. Lis, J. Matuszewski, Acta Crystallogr. B 35 (1979) 2212.
[26] F.S. Delgado, C. Ruiz-Pérez, J. Sanchiz, F. Lloret, M. Julve, Inorg. Chim. Acta, in preparation.